Two-Photon Laser-Induced Reaction of 1,8-Bis(halomethyl)naphthalenes from Different Excited States and Transient Targeting of Its Intermediate by Time-Delayed, Two-Color Photolysis and Argon Ion Laser-Jet Photolysis Techniques

Akihiko Ouchi,*,† Yoshinori Koga,† and Waldemar Adam‡

Contribution from the National Institute of Materials and Chemical Research, AIST, MITI, Tsukuba, Ibaraki 305, Japan, and Institute of Organic Chemistry, University of Würzburg, Am Hubland, D-97074 Würzburg, Germany

Received August 16, 1996[⊗]

Abstract: Two-photon chemistry of 1,8-bis(bromomethyl)naphthalene (**1a**) and 1,8-bis(chloromethyl)naphthalene (**1b**) was studied by (a) laser photolysis with use of XeCl (308 nm), KrF (248 nm), and ArF (193 nm) excimer lasers, (b) time-delayed, two-color photolysis with use of XeCl and XeF (351 nm) lasers, and (c) argon ion laser-jet (333, 351, and 364 nm) photolysis by both direct and benzophenone sensitization. The reaction proceeds through an intermediate monoradical **2**, which is generated by a one-photon process, followed by additional photolysis to the two-photon product acenaphthene (**4**). On excitation of substrate **1** to its S_1 state, monoradical **2** is formed directly from the S_1 state and subsequently from the T_1 state through intersystem crossing, alternatively on benzophenone sensitization. Upper excited states, namely S_2 and S_3, of **1** are proposed in the KrF and ArF excimer laser irradiation, generating intermediate **2** through fast fragmentation of the T(σ*) state. Transient targeting of intermediate **2** by time-delayed, two-color photolysis and argon ion laser-jet photolysis increases considerably the yield of the two-photon product **4**.

Introduction

In spite of the wide application of lasers in spectroscopy and analytical chemistry, comparatively little synthetic work has been done in the field of organic chemistry.[1,2] The most prominent features of a laser are its high intensity, monochromacity, and intermittence in the case of pulsed lasers. Photochemical activation of multifunctional molecules may be carried out by lasers by utilizing the high intensity of the laser. Most of such studies have been carried out for the spectral detection and identification of the short-lived transients involved and the measurement of their kinetics. However, while such spectroscopic studies are, of course, useful to understand multiphoton reactions, they usually provide no information on the products of the photochemical process because the sub-milligram quantities of products that are formed do not allow characterization and quantitative analysis. Nevertheless, to assess complete mechanistic details of a chemical transformation, the kinetics of the process and the detection and identification of the intermediates as well as product studies are indispensable.

Scheme 1

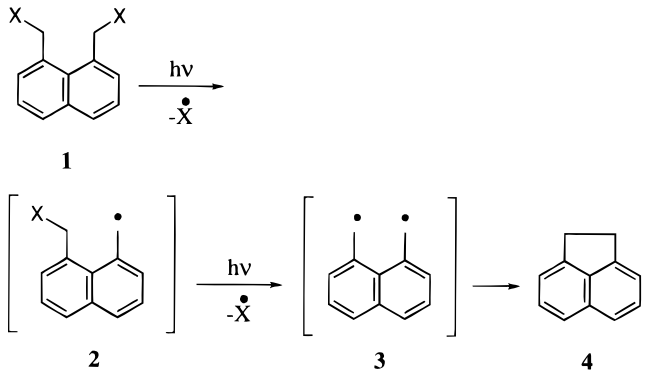

a : X = Br **b** : X = Cl

For the present mechanistic study, we have chosen 1,8-bis(halomethyl)naphthalenes **1** as the substrate and conducted the multiphoton reaction shown in Scheme 1.[3] This class of compounds was chosen because extensive spectroscopic studies have been conducted on the photolysis of monosubstituted analogs, namely the 1-(halomethyl)naphthalenes **5** (Scheme 2),[4] which should provide the necessary background for the mechanistic interpretations of the reactions of the disubstituted derivatives **1**. Analogous to the formation of the 1-naphthylmethyl radical **6** in the laser photolysis of **5**, it was expected that the corresponding naphthylmethyl radicals **2** should be formed in the photolysis of **1**. Subsequent photochemical

† National Institute of Materials and Chemical Research.

‡ Institute of Organic Chemistry.

⊗ Abstract published in *Advance ACS Abstracts,* December 15, 1996.

(1) (a) Kleinermanns, K.; Wolfrum, J. *Angew. Chem., Int. Ed. Engl.* **1987**, *26*, 38−58. (b) Wilson, R. M.; Schnapp, K. A. *Chem. Rev.* **1993**, *93*, 223−249. (c) Johnston, L. J. *Chem. Rev.* **1993**, *93*, 251−266. (d) Wilson, R. M.; Schnapp, K. A.; Hannemann, K.; Ho, D. M.; Memarian, H. R.; Azadnia, A.; Pinhas, A. R.; Figley, T. M. *Spectrochim. Acta, Part A* **1990**, *46*, 551−558. (e) Wilson, R. M.; Adam, W.; Schulte Oestrich, R. *Spectrum.* **1991**, *4*, 8−17.

(2) (a) Wilson, R. M.; Hannemann, K.; Peters, K.; Peters, E.-M. *J. Am. Chem. Soc.* **1987**, *109*, 4741−4743. (b) Netto-Ferreira, J. C.; Wintgens, V.; Scaiano, J. C. *Tetrahedron Lett.* **1989**, *30*, 6851−6854. (c) Bendig, J.; Mitzner, R. *Ber. Bunsen-Ges. Phys. Chem.* **1994**, *98*, 1004−1008. (d) Mathews, M. G.; Wang, Z.; Koplitz, B. *Chem. Phys. Lett.* **1994**, *227*, 633−638.

(3) Preliminary results: (a) Ouchi, A.; Yabe, A. *Tetrahedron Lett.* **1992**, *33*, 5359−5362. (b) Adam, W.; Ouchi, A. *Tetrahedron Lett.* **1992**, *33*, 1875−1878. (c) Ouchi, A.; Yabe, A. *Chem. Lett.* **1995**, 945−946.

S0002-7863(96)02884-3 CCC: $14.00

Scheme 2

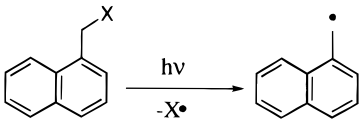

5 **6**

a : X = Br **b** : X = Cl **c** : X = I

activation of the monoradical intermediate **2** should afford the 1,8-naphthalenediylbismethyl **3**.[5] The chemistry of this non-Kekulé species is well-established, which cyclizes to acenaphthene (**4**).[5d,f] In Scheme 1, product **4** derives from a two-photon process and by monitoring its yield, the efficiency of the double activation may be assessed.

The efficiency of the photochemical formation of the monoradical **6** from **5** has been reported to depend on the type of excited state that is involved. Thus, it is anticipated that the efficiency of the two-photon process **1** → **4** will be increased not only by applying high-intensity light for the reaction but also by generating the appropriate excited state, which is accomplished by selecting the proper wavelength in the laser irradiation. In addition, the timing of a second photon absorption by the monoradical intermediate **2** is also expected to be crucial for the effective conversion of **2** → **4** since the generation of **6** from **5** has been reported to proceed from its T_1 state whose lifetime is far longer than the pulse width of an excimer laser. These features are demonstrated in the present quantitative product studies on the multiphoton photolysis of substrates **1a**,**b** by using (a) XeCl (308 nm), KrF (248 nm), and ArF (193 nm) excimer lasers, (b) time-delayed, two-color pulsed photolysis with XeCl and XeF (351 nm) excimer lasers, and (c) argon ion laser-jet photolysis (333, 351, and 364 nm) both by direct and benzophenone sensitization.

Results

Absorption spectra of 1,8-bis(bromomethyl)naphthalene (**1a**), 1,8-bis(chloromethyl)-naphthalene (**1b**), and acenaphthene (**4**) in cyclohexane are shown in Figure 1. The spectra in acetonitrile were almost the same as those in cyclohexane; the shift of the absorption maxima was less than 5 nm. As seen in the spectra, **1a** has its first absorption maximum at 302 nm and the second at 230 nm; similarly, **1b** shows the first absorption maximum at 294 nm and the second at 229 nm. The monosubstituted analogs 1-(bromomethyl)naphthalene (**5a**) and 1-(chloromethyl)naphthalene (**5b**) also possess similar absorption spectra; the absorption maxima of **5a** are located at 291 and 226 nm and those of **5b** at 284 and 224 nm.

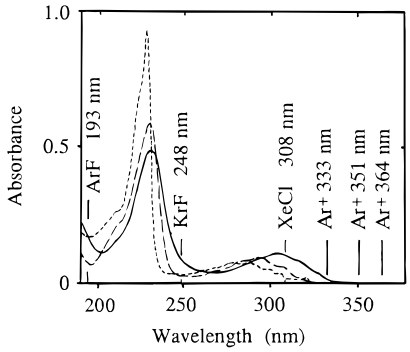

Figure 1. Absorption spectra of 1,8-bis(bromomethyl)naphthalene (**1a**) [—], 1,8-bis(chloromethyl)naphthalene (**1b**) [- - -], and acenaphthene (**4**) [···]. Concentration 10^{-5} M in cyclohexane, optical path 10 mm. The wavelengths of the laser emissions are marked in the figure.

Excimer laser photolyses were conducted in order to study the wavelength and the fluence dependence of **1a**,**b**. Figure 2a,b shows the yield of **4** and the consumption of **1a**,**b** at high (3×10^{22} photon·m^{-2}·pulse^{-1}) excimer laser fluence photolyses as a function of the number of laser shots. As seen in the traces, the conversion of **1a**,**b** depended markedly on the laser that was used. The conversion increased with increasing laser emission wavelength, namely XeCl > KrF > ArF. These results did not simply reflect the absorbance of the substrates because the magnitude of the absorption coefficient at each laser wavelength was ArF > KrF ≈ XeCl for **1a** and ArF > XeCl > KrF for **1b** (*cf.* Figure 1). Although the absorbance of **1b** was smaller than that of **1a**, the conversion rate for **1b** was greater than for **1a** in the XeCl and KrF laser photolyses. In the case of ArF laser photolysis, however, the rate of the consumption of **1a** and **1b** was almost the same.

As shown in Figure 2a,b, the increase in the yield of **4** depended somewhat irregularly on the wavelength of the lasers used, *i.e.*, KrF > XeCl > ArF. This is the result of fluctuations in both the conversion and the efficiency—which is defined as 100 × (yield of **4**)/(conversion of **1**)—at each laser irradiation. The efficiency (Figure 3) of the formation of **4** for the various excimer laser photolyses decreased with increasing laser wavelength, namely ArF > KrF > XeCl. The substrate dependence on the efficiency was **1a** > **1b** in the XeCl and KrF laser photolyses, but it did not change much in the case of the ArF excimer laser photolysis.

Despite the high conversions of **1** for the XeCl and KrF lasers the efficiency and the yield of **4** were low. This may be explained by the coupling of the monoradicals **2** (Scheme 1), which form dimers[4e,g] and possibly oligomeric and polymeric products, as well as by unfavorable secondary reactions of the substrate **1** and the product **4** with the released halogen atoms. Indeed, higher-molecular-weight compounds were observed by TLC analysis of the crude photolysate, as evidenced by considerable amounts of non-eluting products at the origin. As a control experiment, the decomposition of **4** was tested in the high-intensity KrF laser irradiation in the presence and absence of bromine molecules. The results (Table 1) show considerable consumption of **4** in this photolysis, especially in the presence of bromine.

When the irradiations were conducted at medium fluence of the excimer lasers, *i.e.*, 6.2×10^{20} photon·m^{-2}·pulse^{-1} ($^1/_{50}$ of the high-fluence photolyses), the rate of the consumption

(4) (a) Slocum, G. H.; Kaufman, K.; Schuster, G. B. *J. Am. Chem. Soc.* **1981**, *103*, 4625−4627. (b) Kelley, D. F.; Milton, S. V.; Huppert, D.; Rentzepis, P. M. *J. Phys. Chem.* **1983**, *87*, 1842−1843. (c) Gould, I. R.; Tung, C.; Turro, N. J.; Givens, R. S.; Matuszewski, B. *J. Am. Chem. Soc.* **1984**, *106*, 1789−1793. (d) Hilinski, E. F.; Huppert, D.; Kelley, D. F.; Milton, S. V.; Rentzepis, P. M. *J. Am. Chem. Soc.* **1984**, *106*, 1951−1957. (e) Slocum, G. H.; Schuster, G. B. *J. Org. Chem.* **1984**, *49*, 2177−2185. (f) Johnston, L. J.; Scaiano, J. C. *J. Am. Chem. Soc.* **1985**, *107*, 6368−6372. (g) Tolumura, K.; Udagawa, M.; Itoh, M. *J. Phys. Chem.* **1985**, *89*, 5147−5149. (h) Arnold, B.; Donald, L.; Jurgens, A.; Pincock, J. A. *Can. J. Chem.* **1985**, *63*, 3140−3146. (i) Scaiano, J. C.; Johnston, L. J. *Pure Appl. Chem.* **1986**, *58*, 1273−1278. (j) van Haelst, L.; Haselbach, E.; Suppan, P. *Chimia* **1988**, *42*, 231−234. (k) Redmond, R. W.; Wayner, D. D. M.; Kanabus-Kaminska, J. M.; Scaianao, J. C. *J. Phys. Chem.* **1989**, *93*, 6397−6401. (l) Kawai, A.; Okutsu, T.; Obi, K. *Chem. Phys. Lett.* **1990**, *174*, 213−218. (m) Kawai, A.; Okutsu, Y.; Obi, K. *Chem. Phys. Lett.* **1995**, *235*, 450−455.

(5) (a) Gisin, M.; Wirz, J. *Helv. Chim. Acta* **1976**, *59*, 2273−2277. (b) Pagni, R. M.; Burnett, M. N.; Dodd, J. R. *J. Am. Chem. Soc.* **1977**, *99*, 1972−1973. (c) Platz, M. S. *J. Am. Chem. Soc.* **1979**, *101*, 3398−3399. (d) Platz, M. S. *J. Am. Chem. Soc.* **1980**, *102*, 1192−1194. (e) Platz, M. S.; Carrol, G.; Pierrat, F.; Zayas, J.; Auster, S. *Tetrahedron* **1982**, *38*, 777−785. (f) Haider, K.; Platz, M. S.; Despres, A.; Lejenne, V.; Migirdicyan, E.; Bally, T.; Haselbach, E. *J. Am. Chem. Soc.* **1988**, *110*, 2318−2320. (g) Biewer, M. C.; Platz, M. S.; Roth, M.; Wirz, J. *J. Am. Chem. Soc.* **1991**, *113*, 8069−8073.

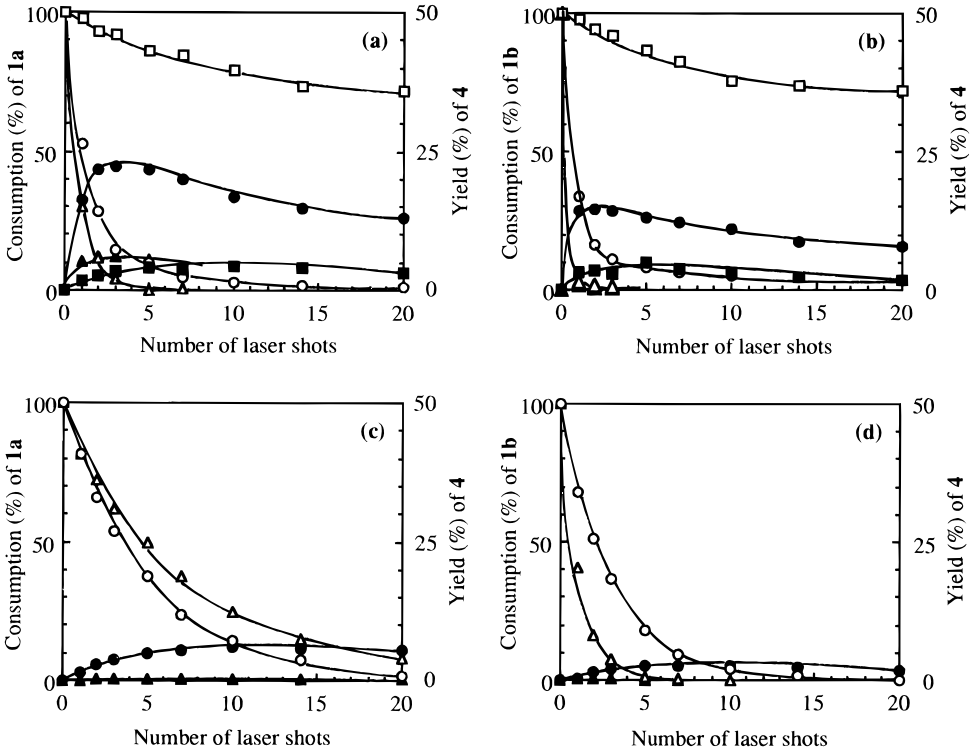

Figure 2. The consumption of substrate **1** (open symbols) and yield of acenaphthene (**4**) (closed symbols) as a function of the number of excimer laser shots. Substrate and fluence of excimer lasers: (a) **1a**, high; (b) **1b**, high; (c) **1a**, medium; (d) **1b**, medium. Eximer lasers: □, ■ (ArF); ○, ● (KrF); △, ▲ (XeCl). Concentration 10^{-5} M in cyclohexane. Fluence of excimer lasers 3.1×10^{22} (high) and 6.2×10^{20} (medium) photon·m^{-2}·pulse^{-1}. The results are the average of two independent runs; the experimental errors are given as Supporting Information.

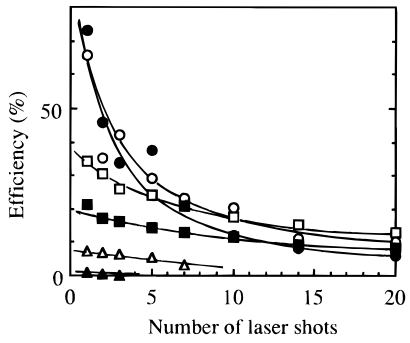

Figure 3. Efficiency of acenaphthene (**4**) formation on irradiation with various high-fluence excimer lasers. Concentration 10^{-5} M in cyclohexane. Fluence of excimer lasers 3.1×10^{22} photons·m^{-2}·pulse^{-1}. Utilized excimer lasers and substrates: ○ (ArF, **1a**); ● (ArF, **1b**); □ (KrF, **1a**); ■ (KrF, **1b**); △ (XeCl, **1a**); ▲ (XeCl, **1b**).

Table 1. Decomposition of Acenaphthene (**4**) by KrF Laser Irradiations[a] in the Presence and Absence of Bromine

	decomposition of **4** (%)	
no. of laser pulses	no additive	with Br_2 (1 equiv)
1	4.7 ± 1.0	15.1
2	11.3 ± 5.1	29.7
3	14.7 ± 3.4	39.1
5	20.0 ± 6.7	45.8
7	23.9 ± 3.6	61.3
10	32.1 ± 5.2	63.5

[a] Fluence: 3.1×10^{22} photon·m^{-2}·pulse^{-1}. Pulse width (fwhm): 30 ns. Concentration: 10^{-5} M in cyclohexane.

decreased for both **1a** and **1b** (Figure 2c,d). The yield of **4** also diminished in the photolyses; for the KrF laser photolysis it dropped to *ca.* $^1/_4$ for **1a** and $^1/_6$ for **1b** compared with those of the high-fluence photolyses. In the case of the XeCl photolyses, practically no acenaphthene was formed for both **1a** and **1b**.

On further decrease of the light intensity, the photolysis became expectedly still less efficient. The low-fluence KrF excimer laser (6.2×10^{18} photon·m^{-2}·pulse^{-1}, $^1/_{100}$ of the medium-fluence photolysis) and the low-pressure mercury lamp (254 nm, 3.4×10^{18} photon·m^{-2}·s^{-1}) photolyses of **1a**,**b** only showed slow consumption of the starting materials and no formation of acenaphthene (**4**).[6]

Time-Delayed, Two-Color Photolyses. This technique involves irradiation with a single XeCl laser pulse (6.2×10^{20} photon·m^{-2}·pulse^{-1}), followed by a time-delayed XeF laser pulse (9.4×10^{20} photon·m^{-2}·pulse^{-1}). The photolysis with the XeF laser alone showed no consumption of **1a**,**b**, which was in accord with the lack of absorption of **1a**,**b** at this wavelength (*cf.* Figure 1). The consumption of **1a**,**b** in the two-color photolysis was independent of the delay times; the average consumption was 29% for **1a** and 91% for **1b** after three sets of two-color irradiations—a set of irradiation comprises a pulse of XeCl and XeF lasers—which were the same as those of the one-color laser photolysis by the XeCl laser. These results indicate that the consumption of **1a**,**b** depends only on the XeCl laser and not on the subsequent XeF laser irradiation.

Figure 4 shows the effect of delay time on the formation of acenaphthene (**4**) in terms of the increment factor, which is defined by $(A - B)/B$, where A is the yield of **4** in the two-color photolysis and B is the yield of **4** in the one-color XeCl laser irradiation. In these figures, an increment factor of 0 means that **4** was formed only by the first XeCl laser and no additional amounts of **4** are produced by the subsequent XeF laser irradiation. In other words, an increment factor >0 indicates additional formation of **4** in the photolysis of an intermediate by the second XeF laser pulse. The expected intermediate is the monoradical **2** with strong absorption at 330−360 nm,[7] similar to that of the parent 1-naphthylmethylradical **6** (*ca.* 340 and 365 nm).[4e,g]

(6) The experimental results are given as Supporting Information.

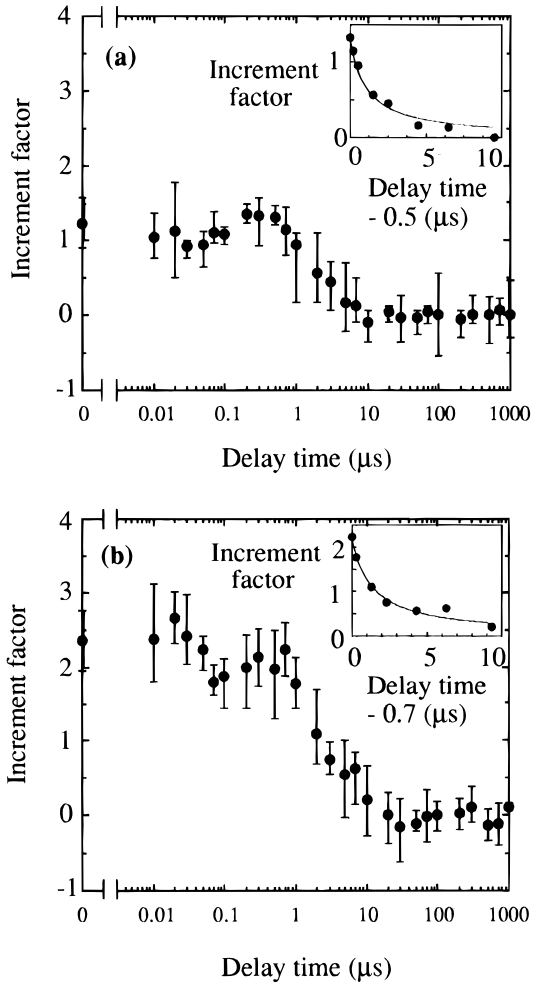

Figure 4. Increment factor for the yield of acenaphthene (**4**) as a function of delay time: (a) from **1a**, (b) from **1b**. Concentration of **1** 10^{-5} M in cyclohexane; laser power of XeCl 6.2 × 10^{20} photons·m^{-2}·$pulse^{-1}$ and of XeF 9.4 × 10^{20} photons·m^{-2}·$pulse^{-1}$. Three sets of two-color irradiations were conducted at each run. The jitter between the two laser pulses is ±3 ns. The results are the average of four independent runs. The insert shows the increment factor in the range of 0.5−10 (a) and 0.7−10 μs (b) with second-order kinetic fitting.

As seen in the traces of Figure 4, the increment factor strongly depends on the delay time. It is significant to note that the increment factor has two maxima for both **1a** and **1b**, the first maximum at 0−30 ns and the second at 0.2−0.5 μs, although the separation of the first and the second maxima of substrate **1a** is not clearly observed. The existence of two maxima suggests the presence of at least two photochemical paths for the formation of **2**.

The yield of acenaphthene (**4**) between 0.5−0.7 and 10 μs delay time followed second-order decay (Figure 4, insert). The result implies that the decrease in the concentration of **2** is due to dimerization, analogous to the related naphthylmethyl radical **6**, for which a second-order decay (dimerization) was reported.[4g] After a delay time of ca. 10 μs, the increment factor decreased to 0, which indicates complete absence of intermediate **2** in this time domain.

Argon ion laser-jet photolyses were conducted for the direct and the triplet-sensitized irradiation under continuous high-intensity conditions. The argon ion laser emits continuously at the three near-UV wavelengths 333, 351, and 364 nm (output energy distribution 1:2:2).

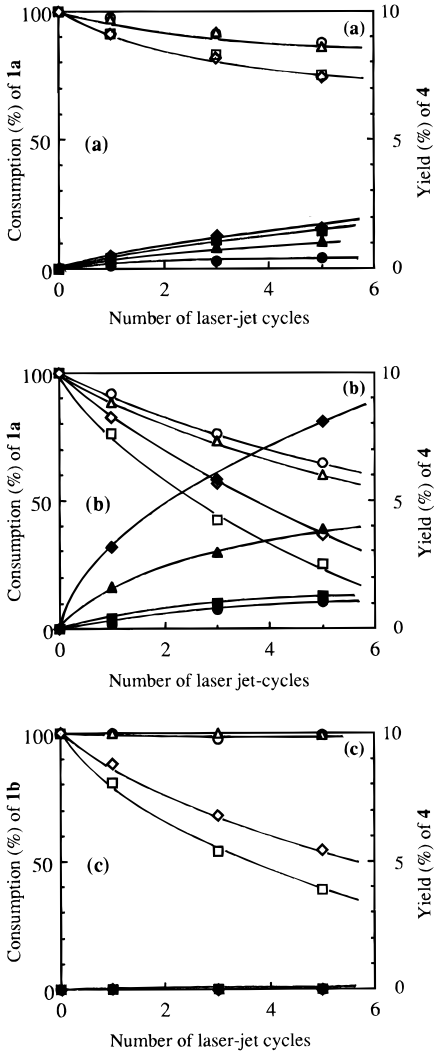

Figure 5. The consumption of **1** (open symbols) and yield of **4** (solid symbols) as a function of the number of laser-jet cycles. Substrate and solvent: (a) **1a**, cyclohexane; (b) **1a**, acetonitrile; (c) **1b**, acetonitrile. Laser power 3.5 W; concentration of **1a** 10^{-4} M; flow rate 2.0 mL·min^{-1}; (i) standard reaction (○, ●), (ii) with 0.1 M **NB** (△, ▲), (iii) with 10^{-3} M **BP** (□, ■), (iv) with 10^{-3} M **BP** and 0.1 M **NB** (◇, ◆). The results are the average of two independent runs; the experimental errors are given as Supporting Information.

In Figure 5a are displayed the results of the laser-jet photolyses in cyclohexane solutions. Four types of laser-jet photolyses were conducted by using all three emissions of the argon ion laser (total output energy 3.5 W): (i) standard irradiation without any additive, (ii) irradiation in the presence of the halogen atom scavenger[8] norbornene (**NB**), (iii) benzophenone (BP)-sensitized irradiation, and (iv) **BP**-sensitized irradiation in the presence of **NB**. As shown in Figure 5a, the addition of the halogen atom scavenger **NB** does not affect the consumption of **1a** but increases the yield of acenaphthene (**4**) both in the direct [type (i) *versus* (ii)] and **BP**-sensitized [type (iii) *versus* (iv)] photolyses. This provides evidence that undesirable side reactions due to the released halogen atoms occur, which decrease the yield of **4**. This is consistent with the results obtained in the excimer laser photolyses (Figure 2 and Table 1). The results for the **BP** sensitization revealed that both the consumption of **1a** and the yield of **4** increase [type (i) *versus* (iii) and (ii) *versus* (iv)].

(7) Ito, O.; Alam, M. M.; Koga, Y.; Ouchi, A. *J. Photochem. Photobiol., A* **1996**, *97*, 19−23.

(8) The effect of other halogen atom scavengers was also studied and the results are given as Supporting Information.

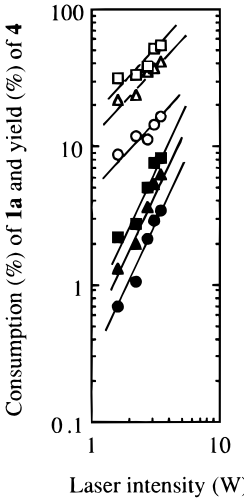

Figure 6. The dependence of the laser intensity on the consumption of **1a** (open symbols) and yield of **4** (closed symbols). Concentrations in acetonitrile: **1a** 10^{-4} M, **BP** 10^{-4} M, **NB** 0.1 M. Flow rate 2.0 mL·min^{-1}. Laser-jet cycles: ○, ● (one); △, ▲ (three); □, ■ (five).

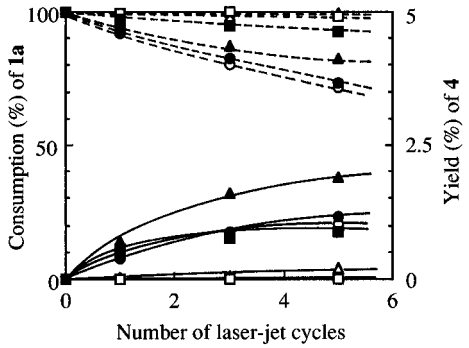

Figure 7. The dependence of the wavelength on the consumption of **1a** (dashed line) and yield of **4** (solid lines). Laser power 3.5 W (total output); **NB**: 0.1 M. Irradiations at (i) 333 nm (○), (ii) 333 nm + 0.1 M **BP** (●); (iii) 351 nm (△), (iv) 351 nm + 0.1M **BP** (▲), (v) 364 nm (□), (vi) 364 nm + 0.1M **BP** (■). The results are the average of two independent runs; the experimental errors are given as Supporting Information.

Laser-jet photolyses were also conducted in acetonitrile under the type (i)−(iv) modes (Figure 5b). A similar trend of reactions was observed compared with those in the cyclohexane solution but with a remarkable increase in both the consumption of **1a** and the yield of **4**; however, a prominent difference is the lower consumption of **1a** in the **BP**-sensitized reaction in the presence of **NB**, although the yield of **4** was increased [type (ii) *versus* (iv)].

For the explicit assessment for the participation of a two-photon process, the intensity effect was studied for the laser-jet photolysis (Figure 6). The consumption of **1a** displayed unit slope for a double-logarithmic plot *versus* light intensity, which indicates that the reaction proceeded by a one-photon process. In contrast, the slope of the yield of **4** of such a plot was 2, which confirms the expected two-photon process.

The effect of each wavelength in the laser-jet photolysis was examined in Figure 7. In the direct photolysis, the consumption of **1a** was only achieved by the 333-nm emission of the laser but not by 351- or 364-nm emissions since substrate **1a** does not absorb at 351 and 364 nm; however, the yield of **4** was low. In contrast, in the BP-sensitized photolyses, consumption of **1a** and the formation of **4** were observed at all three laser lines. The consumption of **1a** in the BP sensitization (at the fifth cycle) was 26% for 333 nm, 18% for 351 nm, and 8% for 364 nm, or a total of 52%, which is similar to the consumption

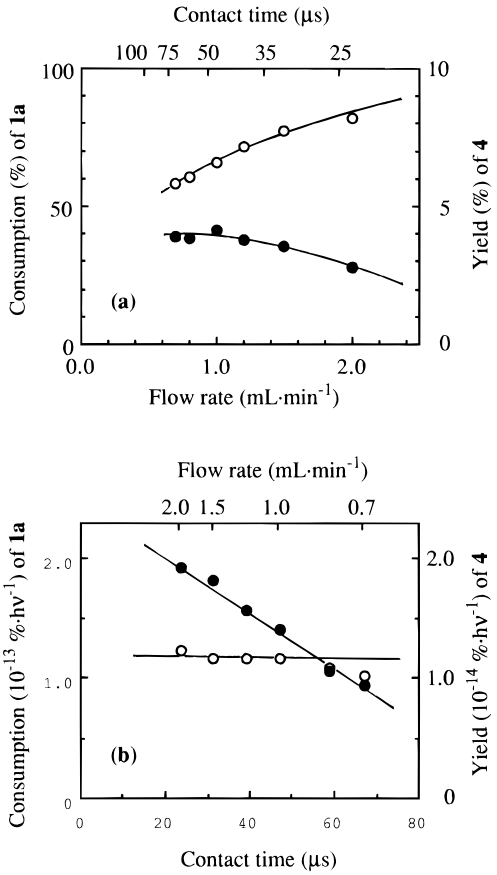

Figure 8. The dependence of the flow rate on (a) the consumption of **1a** and yield of **4** and (b) the consumption of **1a** and yield of **4** per photon: **1a** (○), **4** (●) for one laser-jet cycle. Concentrations in acetonitrile: **1a** 10^{-4} M, **BP** 10^{-4} M, **NB** 0.1 M.

of 61% when all three lines are employed [Figure 5b (iv)]. The slight decrease in the former case is due to the decrease of the laser intensity by using a quartz prism for the separation of the three laser lines. In contrast, the yield of **4** for **BP** sensitization (at the fifth cycle) was 1.2% for 333 nm, 1.9% for 351 nm, and 0.9% for 364 nm, or a total of 4.0%, which is about half of that [8.1%, Figure 5b (iv)] with all three lines.

The dependence on the flow rate of the liquid jet, which corresponds to the contact time of the substrate molecules in the laser beam, is shown in Figure 8, in which the horizontal axis is shown in both flow rate (lower scale) and contact time (upper scale). As seen in Figure 8a, the consumption of **1a** increases with decreasing flow rate, while the yield of **4** levels off at flow rates below 1.2 mL·min^{-1}. In Figure 8b the contact time dependence on the consumption of **1a** and the yield of **4** is displayed but normalized for the number of irradiated photons. As seen in the figure, the consumption per photon is essentially independent of the contact time, which means that the consumption increases linearly with the number of photons; however, the yield of **4** per photon decreased linearly with the contact time, which suggests decomposition of **4** probably by the one-photon process. As a control experiment, the decomposition of substrate **4** by **BP**-sensitized laser-jet photolysis was tested. Indeed, with increasing laser-jet cycles and **BP** concentration, product **4** was more effectively decomposed.[6]

For comparison purpose, the laser-jet photolysis of derivative **1b** was also conducted in acetonitrile for the four reaction types, (i)−(iv), as shown in Figure 5c. Without **BP** no consumption of **1b** was observed in type (i) and (ii) modes, which is in accord with the lack of absorption at the argon ion laser emissions (*cf.* Figure 1). In the case of **BP**-sensitized reactions, types (iii)

Scheme 3

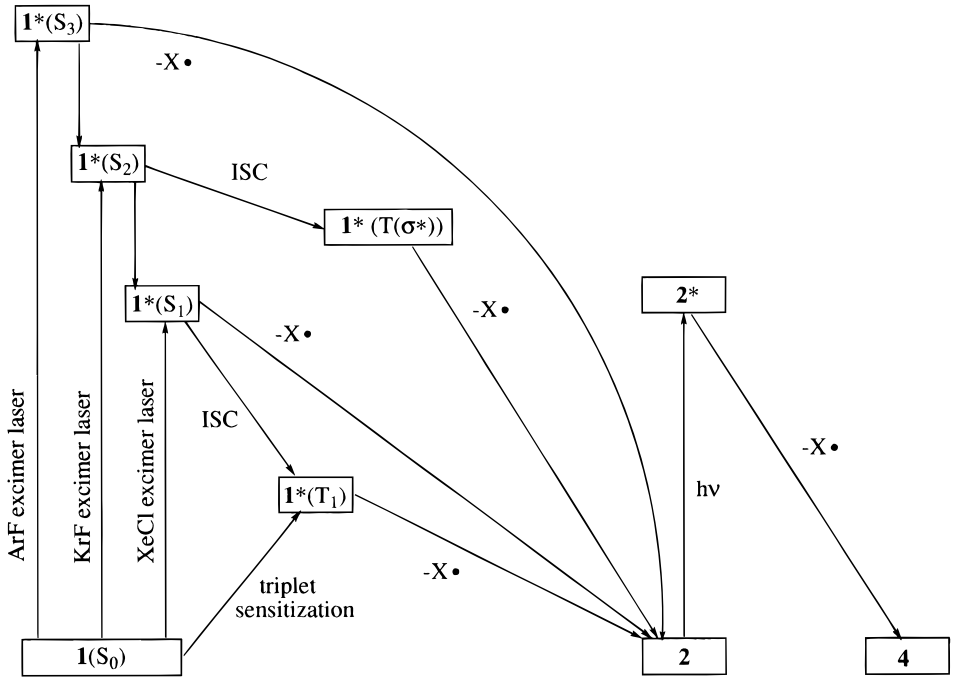

and (iv), consumption of **1b** was observed which was somewhat slower than that of **1a**; however, practically no formation of product **4** was observed in both cases.

Discussion

The results of the direct photolysis can be interpreted in terms of a mechanism established for the monosubstituted substrates **5** (Scheme 2). The first absorption maximum of the monosubstituted analogs, *i.e.*, λ_{max} 291 nm of **5a** and λ_{max} 284 nm of **5b**, by irradiation with a XeCl excimer laser or a nitrogen laser (337 nm), has been reported to involve the excitation to the $S_1(\pi,\pi^*)$ state of the naphthalene ring.[4f] Therefore, the photolysis of **1a**,**b** by a XeCl excimer laser or by the 333-nm emission of the argon ion laser should also proceed through the $S_1(\pi,\pi^*)$ state (Scheme 3). The irradiation to the second maximum of **5a**,**b**, *i.e.*, λ_{max} 226 nm of **5a** and λ_{max} 224 nm of **5b**, by irradiation with the fourth harmonic of a Nd:YAG laser (266 nm) represents the excitation to the $S_2(\pi,\pi^*)$ state.[4b,d] Thus, the photolysis of **1a**,**b** by a KrF excimer laser should also proceed through the $S_2(\pi,\pi^*)$ state of the naphthalene moiety. The type of excitation in the ArF excimer laser irradiation is still not well understood because there are no previous reports on **5a**,**b** which characterize the higher excited states that are produced. However, the excited state is different from the S_1 or S_2 state because the results are different from those of XeCl and KrF laser photolyses (cf. Figures 2 and 3); presumably they are either the $S_3(n,\sigma^*)$ state of the C−X bond[9] or the $S_3(\pi,\pi^*)$ state of the naphthalene ring.

Acenaphthene (4) Formation from the Different Excited States. In the case of the XeCl laser photolysis, substrate **5** is excited to its $S_1(\pi,\pi^*)$ state,[4f,g] whose lifetime is <5 ps for **5a** and 490 ps for **5b**,[10] followed by facile intersystem crossing (ISC) to the $T_1(\pi,\pi^*)$ state.[4f] Substantial homolytic cleavage of the C−X bond in the T_1 state, which has the lifetime of 0.5−0.7 μs,[4f,g] was reported to generate radical **6**.[4l] A similar mechanism is proposed to operate for the disubstituted derivatives **1** to generate intermediate **2** (Scheme 1 and 3), probably with a shorter S_1 lifetime due to the larger heavy atom effect in the facile ISC to the T_1 state; *i.e.*, **1**(S_0) → **1***(S_1) → **1***(T_1) → **2**. Indeed, the existence of the monoradicals **2** is established by the detection of a transient absorption at 330−360 nm in the laser flash photolysis of **1a**,**b**.[7]

An additional photon is necessary for the formation of acenaphthene (**4**), *i.e.*, **2** → **2*** → **4**. This is supported by the fact that with the decrease of the XeCl excimer laser fluence, the decrease on the yield of acenaphthene (**4**) is larger than the decrease in the consumption of **1**. This is also confirmed clearly by the argon ion laser-jet experiments in that the consumption of the substrate followed a one-photon process whereas the formation of acenaphthene required two photons (Figure 6).

In spite of the large consumption of substrate **1**, only a small yield of the two-photon product **4** was obtained in the XeCl excimer laser photolysis. This result can be explained in terms of the time lag between the laser pulse and the formation of intermediate **2**. In view of the fact that the pulse width of the XeCl laser is only 14 ns, which is one order in magnitude shorter than the lifetime of the T_1 state of **1a**,**b**, the monoradicals **2** formed from the T_1 state of substrate **1** in the one-color photolysis have little probability of absorbing a second photon within the same pulse for the formation of the two-photon product **4**. Thus, the monoradical **2** experiences extensive side reactions to afford dimers and higher-molecular-weight products.

In the case of the KrF laser photolysis of **1** (Figure 2), upper excited states are expected in analogy to substrate **5**. When **5** is irradiated by the fourth harmonic of a Nd:YAG laser (266 nm), it is excited to the S_2 state which, in addition to the internal conversion to the S_1 state, leads extremely quickly (within 25 ps, *i.e.*, within the pulse width of the Nd:YAG laser) to *excited* naphthylmethyl radical **6**. The fast formation of the *excited* naphthylmethyl radical **6** derives from ISC of the S_2 to the $T(\sigma^*)$ state, subsequent homolytic cleavage of the C−X bond, and absorption of a second photon by radical **6**. It is likely that such a mechanism also operates for the disubstituted naphthalenes **1** in the KrF laser irradiation (Scheme 3), *i.e.*, **1**(S_0) → **1***(S_2) → **1***[$T(\sigma^*)$] → **2** → **2*** → **4**. The pulse width of 30 ns

(9) (a) Calvert, J. G.; Pitts, J. G., Jr. *Photochemistry*; John Wiley & Sons: New York, 1966; Chapter 5, Section 5−8. (b) Horspool, W.; Armesto, D. *Organic Photochemistry*; Ellis Horwood PTR Prentice Hall: Chichester, 1992; Chapter 6, Section 6.1.

for the KrF excimer laser is long enough for such a two-photon process to occur and a higher yield of product **4** is obtained accordingly.

In the case of ArF laser photolysis, no studies have been conducted with **5** previously. The fact that the results (yield, efficiency, and consumption) are different from those obtained by XeCl and XeF excimer laser photolyses (Figure 2) suggests the participation of an additional reaction path, most likely from higher excited states; however, intermediary states are not clear at present.

The existence of the postulated non-Kekulé type diradical 1,8-naphthalenediylbis(methyl) (**3**)[5] as an intermediate in step **2*** → **4** (in Scheme 3) is still not certain. The absorption spectrum of **3** has been measured in an EPA glass and by flash photolysis of 1-(diazomethyl)-8-methylnaphthalene, which showed several strong absorption maxima in the 300−340-nm region and some weak maxima in the 400−500-nm region.[5g] Our attempt to detect the intermediate **3** in the nanosecond flash photolysis of **1a**,**b** in cyclohexane showed no clear absorption maxima in these wavelength regions.[7] Unfortunately, the transient absorption spectrum of **3** has not been measured in the direct photolysis of **1** in the liquid phase, but its ESR spectrum has been reported during the photolysis of 1,1,2,2-tetrakis(dimethylamino)ethene matrix, probably formed by electron transfer.[5f] An intramolecular radical S_H2-type reaction **2** → **4** is also likely to occur, without the intervention of intermediary diradical **3**.

Transient Targeting of Intermediate 2 by Time-Delayed, Two-Color Photolysis. Although the consumption of **4** was highest for the three excimer lasers used, the disadvantage of the XeCl excimer laser for the formation of acenaphthene (**4**) lies in the time lag between the laser pulse and the formation of intermediate **2**. This disadvantage can be circumvented by applying a second laser pulse when the concentration of intermediate **2** is maximal. Indeed, a substantial increase of the yield of **4** was accomplished in this way (Figure 4).

A significant feature of this method is that the increment factor, *i.e.*, the yield of **4**, reflects the concentration of intermediate **2** at each delay time. Only the intermediate can absorb XeF excimer laser emission and the additional yield of **4** should depend linearly on the concentration of the transient. Figure 4 shows two maxima for the increment factor, the first at 0−30 ns and the second at 0.2−0.5 μs. The second maximum pertains to the monoradical **2** derived from the long-lived T_1 state of **1** through the sequence **1** → **1***(S_1) → **1***(T_1) → **2** → **2*** → **4** (Scheme 3). The delay time of 0.2−0.5 μs at the maximum is in good accord with the expected rise time of the monoradical **2** through the T_1 state, since the lifetimes of the S_1 and T_1 states of the monosubstituted naphthalene **5** are <1 ns[10] and 0.5−0.7 μs.[4f,g] Additional alkyl substitution on radical **6** would be in line with a slight decrease in the T_1 lifetime[11] of **1a**,**b** compared with **5a**,**b**. Additional evidence for the proposed reaction path in Scheme 3 is given by the fact that the second maximum in Figure 4 is higher than the first for **1a**, but *vice versa* for **1b**. This is rationalized in terms of the more efficient population of the T_1 state in the case of **1a** because of more effective ISC **1***(S_1) → **1***(T_1), which is promoted by the heavy atom effect of bromine.

The first maximum observed at very short delay time (0−30 ns) in the time-delayed, two-color photolyses (Figure 4) provides evidence for another path in the formation of the monoradical **2**. The existence of this fast process has not been unequivocally observed spectroscopically for substrates **1** and **5** because of the overlap of the absorption spectra derived from the multiple transient species at the initial stage of the photolysis; however, such a fast process has been proposed through product analysis in the photolysis of **5**,[4e] from which formation of radical **6** directly from the S_1 state was proposed. Therefore, in analogy we suggest that additionally the monoradical **2** is generated from the substrate **1** through the sequence **1**(S_0) → **1***(S_1) → **2** in Scheme 3.

Transient Targeting of Intermediate 2 by Argon Ion Laser-Jet Photolyses. Another way of overcoming the disadvantage of the XeCl excimer laser photolysis is the utilization of high-intensity, continuous light sources so that intermediate **2**, efficiently generated from the $T_1(\pi,\pi^*)$ state, can have sufficient time for the absorption of a second photon. The laser-jet method fulfills this requirement and also has the advantage that the argon ion laser emits continuously at the three wavelengths 333, 351, and 364 nm. The 333-nm emission is suitable for the first and the 351- and 364-nm lines for the second step photolysis (Scheme 1). An additional advantage is that undesirable side reactions of the intermediate monoradical **2** are minimized because of the favorable 1:2:2 intensity distribution of the three wavelengths. Thus, the sum of the 351- and 364-nm emissions is better than 4-fold more intense than the 333-nm emission and the monoradical **2** is photochemically more quickly consumed at the 351- and 364-nm wavelength than generated at the 333-nm wavelength and thereby prevented from accumulating sufficiently for bimolecular side reactions (dimerization).

Indeed, although the fluence (7.9×10^{26} for the laser-jet *versus* 4.5×10^{28} photon·m^2·s^{-1} for the XeCl excimer laser) and the number of photons per contact (1.5×10^{14} photon·cycle^{-1} for the laser-jet *versus* 6.3×10^{16} photon·pulse^{-1} for the XeCl excimer laser) of the argon ion laser-jet were $^1/_{57}$ and $^1/_{420}$ of that of the medium fluence XeCl excimer laser, an ca. 4.5-fold increase in the yield of **4** (at 36−38% conversion of **1a**) during the photolysis in cyclohexane was observed in the argon ion laser-jet [Figure 5a, type (i)] compared with the medium fluence XeCl excimer laser (Figure 2). Furthermore, the actual increase of the yield of **4** is expected to be higher than 4.5-fold because the laser-jet experiments were conducted at 10-fold higher concentration of **1a** than those of the XeCl excimer laser photolyses. In this context, it has been reported that the yield of **4** decreased with the increase of the substrate concentration.[12]

Further increase in the consumption of **1a** and the yield of acenaphthene (**4**) was accomplished by the **BP** sensitization [Figure 5a, type (i) *versus* (iii)]. This is due to the more efficient formation of intermediate **2** through the **1***(T_1) state. In the direct photolysis, as shown in Figure 7, the excitation is only accomplished by the 333-nm emission whose energy is merely 20% of the total output. In contrast, for the BP sensitization the 351- and 364-nm emissions of the argon-ion laser generate also the intermediate **2** through the **1***(T_1) state in addition to the 333-nm emission. The change of solvent from cyclohexane to acetonitrile showed significant increase of the yield and consumption in the reaction (Figure 5a *versus* Figure 5b). The results can be rationalized by the facility of the halogen atom escape from the solvent cage[13] or by the participation of

(10) Huppert, D.; Rand, S. D.; Reynolds, A. H.; Rentzepis, P. M. *J. Chem. Phys.* **1982**, *77*, 1214−1224.

(11) Carmichael, I.; Hug, G. L. *Handbook of Organic Photochemistry*; Scaiano, J. C., Ed.; CRC Press: Boca Raton, 1989; Vol. I, Chapter 16.

(12) In the case of the medium- and high-fluence KrF excimer laser photolysis of **1a**, the yield of **4** decreased to 1/75 when the concentration of **1a** was changed from 10^{-5} to 10^{-3} M.[6]

(13) The fraction of escaped radical pairs from the cage is a linear function of $(1/\eta)^n$, where η is the viscosity of solvent and n is a value between 0.5 and 1.[16] The viscosity of cyclohexane is 0.608 cP (30 °C) and that of acetonitrile is 0.325 cP (30 °C).[17] Therefore, the escape of halogen atoms will be larger in acetonitrile than in cyclohexane so that the higher consumption of **1** and the yield of **4** should be observed.

additional ionic reaction paths;[14] however, the explicit reason for this solvent effect is not clear at present.

Conclusions

The laser chemistry of 1,8-bis(bromomethyl)naphthalene (**1a**) and 1,8-bis(chloromethyl)naphthalene (**1b**) proceeds through an intermediate monoradical **2**, which is generated by a one-photon process (Scheme 1), followed by successive photolysis of **2** to afford the two-photon product acenaphthene (**4**). The yield of two-photon product **4** was optimized by means of time-delayed, two-color photolysis and argon ion laser-jet photolysis, the latter by direct and benzophenone sensitization; significant increase in the yield of product **4** was observed in both photolysis techniques. On excitation to the S_1 state by using the XeCl excimer laser, the monoradical **2** was formed directly from the S_1 state and also from the T_1 state, which was generated by ISC from the S_1 state. Participation of higher excited states is also proposed, *e.g.*, population of the S_2 state by irradiation with the KrF excimer laser, in which presumably fast C−X homolysis though the T(σ*) state generates the monoradical intermediate **2**.

Experimental Section[15]

Excimer Laser Photolyses. These reactions were conducted in cyclohexane solution under a nitrogen gas atmosphere. High-intensity photolyses (3.1×10^{22} photon·m^{-2}·pulse^{-1}) were conducted by using an ca. 1.5-cm capillary of 1-mm diameter, one of whose ends was closed. A 10-μL aliquot of the solution was placed into a horizontally placed capillary and the laser light was focused at the opening of the capillary, at which a stream of nitrogen gas was directed. Medium- and low-intensity photolyses (6.2×10^{20} and 6.2×10^{18} photon·m^{-2}·pulse^{-1}) were conducted on 0.5−1.0-mL solution under a nitrogen gas atmosphere by using a synthetic quartz cuvette of 10-mm width and 10-mm optical path. For the irradiations, the excimer lasers used were Lambda Physik EMG 102 [pulse width (fwhm) 14 ns (XeCl)] and Lambda Physik EMG 201 [pulsewidth (fwhm) 23 ns (ArF, typical), 30 ns (KrF), and 26 ns (XeF)]. The pulse energy was measured by means of a Gentec joulemeter ED-500 and a Tektronix T912 10MHz storage oscilloscope.

Time-Delayed, Two-Color Photolyses. These reactions were conducted on 0.5 mL of 10^{-5} M cyclohexane solutions under a nitrogen gas atmosphere by using a synthetic quartz cuvette of 10-mm width and 10-mm optical path. The first pulse was generated by a Lambda Physik EMG 102 [XeCl, 6.2×10^{20} photon·m^{-2}·pulse^{-1}, pulse width (fwhm) 14 ns] and the second pulse by a Lambda Physik EMG 201 [XeF, 9.4×10^{20} photon·m^{-2}·pulse^{-1}, pulse width (fwhm) 26 ns] excimer laser. The pulse energy was measured by means of a Gentec joulemeter ED-500 and a Tektronic T912 10MHz storage oscilloscope. The delay times between the two laser pulses were controlled by a four-channel digital delay/pulse generator (Stanford Research Systems Inc., Model DG535). The delay times of the two laser pulses were measured with a biplaner photoelectric tube (Hamamatsu Photonics K. K., model R1193U-05) and a storage scope (Iwatsu Electric Co. Ltd., model TS-8123).

Argon Ion, Laser-Jet Photolyses. These photolyses were conducted under an argon gas atmosphere by using the reported apparatus.[1d,e] The argon ion laser was an Innova 100-20 system from Coherent [output energy distribution 333 (20%), 351 (40%), and 364 nm (40%)] and the laser was focused by a quartz convex lens ($f = 80$ mm). The laser output was 3.5 W, whose fluences at each emission (photons·m^{-2}·s^{-1}) were 1.5×10^{26} for 333 nm, 3.1×10^{26} for 351 nm, and 3.3×10^{26} for 364 nm. In some experiments, the three emissions of the laser were separated by means of a quartz prism. The solutions were prepared by dissolving the substrate in an appropriate solvent and norbornene was added in some experiments. The sensitized photolyses were conducted with benzophenone as the triplet sensitizer. The solution was cycled through the apparatus for 30 to 60 min under an argon gas atmosphere before photolysis in order to eliminate the dissolved oxygen in the solution. The diameter of the capillary in the laser-jet apparatus was 100 μm and the specified flow rate was controlled by means of a Bischoff HPLC 2200 pump.

Analysis of the Photolysis Products. The yield of the two-photon product, namely acenaphthene (**4**), and the consumption of the starting material were determined by HPLC analysis on a Merck Supersphere 60 RP-8 column (244 mm × 4 mm i.d.) and their retention times compared with the authentic samples. The HPLC system consisted of a JASCO TRI Rotar-V HPLC pump and a JASCO 870-UV UV/VIS detector, or a Shimadzu LC-6A HPLC pump and a Shimadzu SPD-6AV UV-Vis spectrometric detector.

Acknowledgment. We thank the Deutsche Forschungsgemeinschaft, the Fonds der Chemischen Industrie, and the Agency of Industrial Science and Technology (MITI, Japan) for financial support. A.O. expresses his gratitude to the Alexander von Humboldt Foundation for a research fellowship (1991).

Supporting Information Available: Preparation of compounds **1a**,**b**. Experimental errors in Figures 2, 5, and 7; photolysis of **1a**,**b** by low-fluence KrF and KrCl excimer lasers, and low-pressure mercury lamp; substrate concentration effect on the high- and medium-fluence KrF excimer laser photolyses of **1a**,**b**; dependence on the benzophenone concentration and halogen atom scavengers in the argon-ion laser-jet photolysis of **1a**; decomposition of **4** by benzophenone-sensitized argon-ion laser-jet photolysis (12 pages). See current masthead page for ordering and Internet access instructions.

JA962884L

(14) In addition to a radical reaction path, the presence of an ionic path has been reported in the photolysis of **5** in methanol: ref 4e.

(15) Preparation of compounds **1a**,**b** is given as Supporting Information.

(16) Leffler, J. E. *An introduction to free radicals*; John Wiley & Sons: New York, 1993; Chapter 4, Section 4.2.2.

(17) Riddick, J. A.; Bunger, W. B. *Techniques of Chemistry, Organic Solvents*, 3rd ed.; Wiley-Interscience Publication, John Wiley & Sons: New York, 1970; pp 139 and 399.